

This discussion paper is/has been under review for the journal Biogeosciences (BG).
Please refer to the corresponding final paper in BG if available.

The keystone species of Precambrian deep bedrock biosphere belong to *Burkholderiales* and *Clostridiales*

L. Purkamo¹, M. Bomberg¹, R. Kietäväinen², H. Salavirta¹, M. Nyssönen¹,
M. Nuppenen-Puputti¹, L. Ahonen², I. Kukkonen^{2,a}, and M. Itävaara¹

¹VTT Technical Research Centre of Finland Ltd., Espoo, Finland

²Geological Survey of Finland (GTK), Espoo, Finland

^anow at: University of Helsinki, Helsinki, Finland

Received: 13 September 2015 – Accepted: 23 October 2015 – Published: 11 November 2015

Correspondence to: L. Purkamo (lotta.purkamo@vtt.fi)

Published by Copernicus Publications on behalf of the European Geosciences Union.

18103

Abstract

The bacterial and archaeal community composition and the possible carbon assimilation processes and energy sources of microbial communities in oligotrophic, deep, crystalline bedrock fractures is yet to be resolved. In this study, intrinsic microbial communities from six fracture zones from 180–2300 m depths in Outokumpu bedrock were characterized using high-throughput amplicon sequencing and metagenomic prediction. *Comamonadaceae*-, *Anaerobrancaceae*- and *Pseudomonadaceae*-related OTUs form the core community in deep crystalline bedrock fractures in Outokumpu. Archaeal communities were mainly composed of *Methanobacteraceae*-affiliating OTUs. The predicted bacterial metagenomes showed that pathways involved in fatty acid and amino sugar metabolism were common. In addition, relative abundance of genes coding the enzymes of autotrophic carbon fixation pathways in predicted metagenomes was low. This indicates that heterotrophic carbon assimilation is more important for microbial communities of the fracture zones. Network analysis based on co-occurrence of OTUs revealed the keystone genera of the microbial communities belonging to *Burkholderiales* and *Clostridiales*. Bacterial communities in fractures resemble those found from oligotrophic, hydrogen-enriched environments. Serpentinization reactions of ophiolitic rocks in Outokumpu assemblage may provide a source of energy and organic carbon compounds for the microbial communities in the fractures. Sulfate reducers and methanogens form a minority of the total microbial communities, but OTUs forming these minor groups are similar to those found from other deep Precambrian terrestrial bedrock environments.

1 Introduction

The microbial communities in deep terrestrial subsurface biosphere contribute significantly to the overall biomass on Earth (Whitman et al., 1998; McMahon and Parnell, 2014). It is essential to understand the metabolic capacity and energy sources of the

18104

microbial communities in deep biosphere in order to evaluate their role in global biogeochemical cycles, assess the risks these communities might cause to for example geological long-term storage of nuclear waste, and even to estimate the possibility of microbial life in deep subsurface of other planetary bodies. In general, chemolithoautotrophic organisms are thought to be the primary producers in deep crystalline rock environments, into which sunlight, or the organic carbon or oxygen produced in photosynthesis, do not penetrate (Gold, 1992; Pedersen, 1997, 2000). Therefore, energy and carbon sources for deep biosphere have to be geochemical. The most important source of reducing power in deep subsurface is H₂. It is produced in abiotic reactions such as through radiolysis of H₂O, water-rock interactions such as serpentinization, but also by microbial activity (Pedersen, 2000; Lin et al., 2005; McCollom, 2013; Szponar et al., 2013). Carbon sources for microbes in deep subsurface are usually in the form of CO₂, CH₄ or other small hydrocarbons. Abiotic synthesis of organic carbon may take place through Fischer–Tropsch type reactions and provide a photosynthesis-independent carbon source for heterotrophic organisms in deep terrestrial biosphere (Proskurowski et al., 2008; McCollom et al., 2010; Etiope and Sherwood Lollar, 2013; Kietäväinen and Purkamo, 2015). This process may be triggered and enhanced by continuous H₂ flux provided by for example serpentinization. Numerous studies have characterized microbial communities of deep Precambrian rock formations (e.g. Pedersen et al., 1996, 2008; Hallbeck and Pedersen, 2008, 2012; Lin et al., 2006; Gihring et al., 2006; Silver et al., 2010; Itävaara et al., 2011; Nyysönen et al., 2012; Purkamo et al., 2013, 2015; Osburn et al., 2014; Bomberg et al., 2015a, b). Although some of these studies have explored the energy and carbon sources or electron accepting processes in these environments, attention has been focused mainly on chemoautotrophic organisms utilizing H₂ and CO₂. After all, abiotic synthesis of organic carbon could also provide a photosynthesis-independent source of carbon and thus support heterotrophic organisms in deep biosphere (Amend and Teske, 2005; Schrenk et al., 2013). However, heterotrophic involvement to the carbon cycling and energy production in the deep continental bedrock biosphere has been rather neglected (Amend and Teske, 2005),

18105

although it was recently suggested that heterotrophy might play a significant role in deep fluids of Fennoscandian crystalline rock (Purkamo et al., 2015).

While the microbial communities in deep marine subsurface environments have been intensively characterized within the last decade with next-generation sequencing methods (Sogin et al., 2006; Biddle et al., 2008, 2011; Brazelton et al., 2012), high-throughput (HTP) sequencing techniques have only recently emerged in characterization of the terrestrial deep subsurface microbial communities (Nyysönen et al., 2014; Bomberg et al., 2014, 2015a, b; Lau et al., 2014; Mu et al., 2014). Vast amount of data obtained from HTP sequencing studies can be used to estimate ecological measures such as species richness, abundance and β -diversity, but it also allows the exploration of significant relationships between microbial taxa and their coexistence in a specific environment (Zhou et al., 2011; Barberan et al., 2012; Lupatini et al., 2014). These co-occurrence patterns, i.e. interactions between different microbial taxa and the complexity of the microbial communities can significantly contribute to the processes that will take place in the ecosystem (Zhou et al., 2011). In addition, keystone organisms can be identified from co-occurrence patterns of the community. Keystone organisms often have a greater role in the ecosystem functionality than their abundance refers (Power et al., 1996). For example, in hydrogen-driven lithoautotrophic ecosystems, autotrophic methanogens can be responsible of primary production of the whole ecosystem (Pedersen, 2000; Nealson et al., 2005). Moreover, these diverse minority groups with low abundance, i.e. the so-called rare biosphere, can be an almost infinite source of genetic potential to be distributed through the microbial populations via gene transfer (Sogin et al., 2006).

In this study, high-throughput amplicon sequencing, metagenome prediction and co-occurrence analysis were used (1) to describe the microbial community structure, (2) to detect key microbial genera of deep fracture fluids in Outokumpu, (3) to evaluate the possible carbon assimilation processes taking place in deep bedrock and ultimately, (4) to understand the origin of carbon and energy sources in Outokumpu Palaeoproterozoic deep bedrock and to establish links between microbial communities and

18106

the geology and geochemistry in Outokumpu crystalline rock biosphere. Groundwater samples were collected from six different fracture zones located at depths ranging from 180 to 2300 m, and bacterial and archaeal communities in these fractures were characterized by their 16S rRNA genes and transcripts. In addition, two functional groups carrying out important electron accepting processes in deep subsurface, namely sulphate reduction and methanogenesis were characterized by dissimilatory sulfite reductase and methyl-coenzyme M reductase genes, respectively.

2 Materials and methods

2.1 Sample collection and geochemistry

Deep subsurface fracture fluids were collected during years 2009–2011 from the Outokumpu Deep Drill Hole, Eastern Finland. The sampling was conducted from overall six depths, 180, 500, 967, 1820, 2260 and 2300 m, as described previously (Purkamo et al., 2013). Shortly, 967 m and shallower depths were packer-isolated and purged for 21–42 days, and deeper fractures were sampled with slow continuous pumping of the fluid from the fracture depth for 9–63 days in order to flush the drill hole. Care was taken to ensure that the pumping rate did not exceed the rate of inflow from the fracture zone. The hydrogeological characteristics of these fluids differ with depth (Table 1). Kietäväinen et al. (2013) described five different water types in Outokumpu, and the fracture zones in this study represent the types I (180 m), II (500 and 967 m), IV (1820 and 2260 m) and V (2300 m). The type I water is characterized with high pH (around 10) and higher alkalinity than other water types in Outokumpu. High pH in the drill hole water column probably originates from cementation within the uppermost 200 m of the drill hole, while during long-term pumping of the 180 m fracture zone, pH dropped to the level of 8.5. Water type II contains the highest amount of dissolved gases in the whole water column, of which approximately 75 % (22–32 mmolL⁻¹) is methane. Distinctive greenish colour and unpleasant “rotten egg” odour are typical for water type IV, indi-

18107

cating presence of reduced sulfur compounds. Water type V also has special features, such as high K and Li concentration due to the interaction with surrounding granitic rocks. In addition, the dominant dissolved gases in the two deepest water types IV and V are He and H₂, in contrast to the CH₄-dominated water types above 2 km depth (Kietäväinen et al., 2013).

The fluid from each fracture zone was collected in the field into sterile, acid-washed glass bottles (Schott) in an anaerobic chamber (MBraun, Germany). The anaerobic conditions in the chamber were achieved as previously described (Purkamo et al., 2013). The biomass for RNA and DNA extraction was collected on nitrocellulose acetate filters (Corning Inc., NY, USA) from 3 × 1 and 3 × 0.5 L of fracture fluid by vacuum suction. The filter was cut from the filter funnel with sterile scalpel and placed immediately to dry ice in a sterile 50 mL plastic tube (Corning Inc., NY, USA). In the laboratory, the samples were preserved at –80 °C before processing. In addition, duplicate 100 mL fluid samples for microbial cell enumeration were obtained from each fracture zone. Sterile, acid-washed 120 mL serum bottles were flushed with a small amount of fracture fluid in the anaerobic cabinet and subsequently filled with 100 mL of the sample fluid, capped with butyl rubber stoppers, sealed with aluminium crimp caps and kept refrigerated until further processing in the laboratory within five days after the sampling.

2.2 Enumeration of the total amount of microbes

In order to calculate the total amount of microbes in fracture fluids, microbes were stained with 4'-6-diamidino-2-phenylindole (DAPI). Preparation of the duplicate samples for examination by microscopy was conducted as in Purkamo et al. (2013). Stained microbes were collected from 5 mL fracture fluid samples by filtering, rinsed and filter was placed on microscopy slide. The total cell number in the samples was based on the sum of counted cells and the effective area of the filter divided by volume of filtrated sample, number of randomly selected microscopy fields and the surface area of the field at 100× magnification.

18108

2.3 Nucleic acids preparation

DNA and RNA were extracted from the biomass with PowerSoil DNA or PowerWater RNA extraction kit (MO BIO Laboratories, Inc., CA, USA) as previously described (Purkamo et al., 2013). An additional DNase treatment was applied to RNA extracts that had DNA contamination detected by PCR performed with P1 and P2 primers for bacterial 16S rRNA gene (Muyzer et al., 1993) as previously described in Purkamo et al. (2013). RNA was reverse-transcribed in triplicate reactions with random hexamers using the Superscript III Reverse Transcriptase kit (Invitrogen, ThermoFisherScientific, MA, USA) as described in Purkamo et al. (2013). The triplicate reactions were pooled and subsequent cDNA as well as DNA were stored at -80°C . Negative controls for reagents were included in every extraction and translation step.

2.4 Quantitative estimation of bacterial and archaeal communities

The bacterial and archaeal numbers in each fracture were estimated with quantitative PCR from DNA extracts. 16S rRNA gene copy number was used as a proxy of the quantity of bacteria and archaea. In addition, qPCR was conducted to calculate the abundance of genes representing the key metabolic processes in anaerobic subsurface environments, namely sulfate reduction and methanogenesis with dissimilatory sulphite reductase (*dsrB*) and methyl-coenzyme M reductase (*mcrA*) genes, respectively. Bacterial 16S rRNA gene copy numbers were determined with V3 region-targeted primers P1 and P2 (Muyzer et al., 1993) resulting in a 190 bp product. A 370 bp fragment of *dsrB* gene and transcript was amplified with the primer pair DSRp2060f and DSR4R (Wagner et al., 1998; Geets et al., 2006). Archaeal 16S rRNA genes were amplified with ARC344f (Bano et al., 2004) and Ar774r (modified from Barns et al., 1994) primers producing a 430 bp product. A 330 bp fragment of *mcrA* gene was amplified with the primer pair ME1 and ME3rc (Hales et al., 1996; Nyysönen et al., 2012).

Bacterial 16S rRNA gene-targeted qPCR was performed in triplicate reactions of each sample with KAPA™ SYBR® Fast 2x Master mix for Roche LightCycler 480 (Kapa

18109

Biosystems, Inc., MA, USA) and $0.3\ \mu\text{M}$ each of forward and reverse primer. The qPCR was performed on a Roche LightCycler 480 (Roche Applied Science, Germany) on white 96-well plates (4titude, UK) and sealed with transparent adhesive seals (4titude, UK). The qPCR conditions consisted of an initial denaturation at 95°C for 10 min followed by 45 amplification cycles of 15 s at 95°C , 30 s at 55°C and 30 s at 72°C and a final extension step of 3 min at 72°C . After the quantification analysis, the melting curves for each reaction were determined. The melting curve analysis consisted of a denaturation step for 10 s at 95°C followed by an annealing step at 65°C for 1 min prior to a gradual temperature rise to 95°C at a rate of $0.11^{\circ}\text{C s}^{-1}$ during which the fluorescence was continuously measured. Amplification of *dsrB*, archaeal 16S rRNA and *mcrA* genes were performed in triplicate for each sample as described in Purkamo et al. (2013), Bomberg et al. (2015b) and in Nyysönen et al. (2014), respectively. The gene copy numbers were calculated by comparing the amplification result to a standard dilution series. Bacterial 16S rRNA and *dsrB* gene copy numbers were determined in each sample by comparing the amplification result to a standard dilution series ranging from 0 to 10^7 of plasmid DNA containing *Escherichia coli* ATCC 31608 or from 1.5×10^1 to 1.5×10^7 copies of *Desulfobulbus propionicus* DSM 2554 *dsrB* gene, respectively. Archaeal 16S rRNA and *mcrA* gene copy numbers were determined by comparing the amplification result to a dilution series of genomic DNA of *Halobacterium salinarum* DSM 3754 or to 5 to 5×10^6 copies of *Methanothermobacter thermautotrophicus* DSM 1053 *mcrA* gene, respectively. No-template controls as well as nucleic acid extraction and translation reagent controls were analysed with the corresponding samples in the same run. The inhibition effect of the samples was evaluated by mixing a specified amount of standard dilution to each sample DNA or cDNA. Spiked reactions were then subsequently amplified using the same protocols as described above. The inhibition in each sample could be evaluated by comparing the amplification efficiency of the sample-spiked standard DNA to the corresponding standard dilution quantity in the standard curve. Inhibition was found to be low in all samples (data not shown).

18110

2.5 High-throughput amplicon sequencing

PCR amplicon libraries from hypervariable region V1-V3 of bacterial 16S rRNA gene were generated with barcoded 8f and P2 primers (Edwards et al., 1989; Muyzer et al., 1993). Amplification of the *dsrB* gene fragment for dissimilatory sulphate reduction was done with 2060f and 4R primers with barcode sequences (Wagner et al., 1998; Geets et al., 2006). Archaeal libraries were produced with nested PCR method, first using A109f and A915r primers (Großkopf et al., 1998 and Stahl and Amann, 1991, respectively) to amplify ca. 800 bp long fragment of the archaeal 16S rRNA gene and using the resulting product as template in PCR reaction with barcoded A344f and A744 primers (Bano et al., 2004 and modified from Barns et al., 1994, respectively). *McrA* amplicons were also produced with nested PCR, first applying *mcrA*463f and *mcrA*1615r primers (Nyyssönen et al., 2012) and secondly barcoded primers Me1 and Me3 (modified from Hales et al., 1996). PCR reaction mix composed of one unit of proofreading Phusion DNA Polymerase (ThermoScientific), 1× high fidelity buffer and dNTP mix (2.5 mM each), filled to 50 µL with molecular biological grade H₂O. Dimethyl-sulfoxide was used in all PCR reactions to enhance the template availability to polymerase. The amplification cycle consisted of an initial denaturation at 98 °C for 30 s, 35 (bacteria and *dsrB*) or 40 (archaea and *mcrA*) times repetition of 10 s at 98 °C, 15 s at 55 °C and 30 s at 72 °C, and a final extension step of 5 min at 72 °C. Three samples were used for each fracture zone community (RNA or DNA) and two amplification reactions of each sample replicate, thus resulting to maximum of six positive reactions (verified with agarose gel electrophoresis). Successful reactions were pooled prior to sequencing. PCR reactions were performed also for nucleic acid extraction and reagent control samples. The sequencing of the 180 m samples was performed at Research and Testing Laboratory (Texas, USA) and the rest of the samples, at the institute of Biotechnology (Helsinki, Finland) using the FLX 454 Titanium – platform (454 Life Sciences, Branford, CT, USA).

18111

2.6 Quality control, classification and phylogenetic analysis of sequences

Sequences were analyzed using mothur (v. 1.32.1) (Schloss et al., 2009) and QIIME programs (MacQIIME v. 1.7.0, Caporaso et al., 2010). The QIIME pipeline was used with 16S rRNA gene sequences and mothur with the functional gene sequences. In QIIME, sequences were compared against Greengenes representative OTU set version gg_13_8 with 97 % similarity and the taxonomy was assigned with RDP. With 16S rRNA sequences, the quality score window was set to 50 and sequences shorter than 360 and longer than 450 base pairs were discarded. The proximal primer sequences were allowed to have two or six nucleotide mismatches for bacterial and archaeal sequences, respectively. The high mismatch rate allowed for archaeal sequences was due to an extra guanine nucleotide in the primer sequence of the 500 m sample. Sequences of the functional genes representing sulphate reducers (*dsrB*) and methanogens (*mcrA*) were analyzed with mothur. Raw flowgrams were denoised with the PyroNoise algorithm to reduce PCR and sequencing noise in the data (Quince et al., 2009). All *dsrB* sequences shorter than 200 bp were discarded and no mismatches in the forward primer sequence were allowed. The length limit for *mcrA* sequences was set to 100 bp and four mismatches in primer sequence were allowed due to ambiguous bases in the primer sequence. The resulting sequences were further aligned with model alignments of *dsrB* and *mcrA* sequences from the Fungene repository (Fish et al., 2013) and sequences were assigned to OTUs with nearest neighbour clustering method. Final phylogeny of the representative OTUs was done using the Geneious Pro software package, version 6.1.7 (Biomatters Inc., New Zealand) and blastn and blastx for comparison of the representative OTU sequences to NCBI's databases (Altschul et al., 1990). All sequence data were uploaded to ENA database with accession numbers ERS846377-ERS846388 (bacteria), ERS846389-ERS846397 (archaea), ERS846399-ERS846407 (*dsrB*) and ERS846408-ERS846414(*mcrA*).

18112

2.7 Ecological indices and statistical analyses

Chao1 richness estimates were calculated for the bacterial and archaeal communities with 97 % sequence similarity using the `alpha.diversity.py` command in QIIME. The estimates of diversity, richness and rarefaction were calculated from random subsample of 3030 sequences per sample for bacteria and 270 sequences per sample for archaea. Same α -diversity estimates for *dsrB* and *mcrA* datasets were calculated in mothur from subsamples of 115 and 1712 sequences, respectively. Due to the low amount of *dsrB* sequences (47) retrieved from the 180 m fracture, these data were not subsampled. The bacterial and archaeal OTUs with resolved taxonomy were compared to the hydrogeochemical data as well as to the lithology of each fracture zone. Canonical correspondence analysis was performed with Past3 to the environmental metadata and taxonomical OTU matrix with all archaeal OTUs and bacterial OTUs with more than 0.1 % abundance in the fracture communities (Hammer and Harper, 2001).

2.8 Prediction of functionality and co-occurrence analysis

De novo OTUs were removed from the 16S rRNA OTU taxonomy file (.biom-table) prior to uploading to the Galaxy pipeline for PICRUSt analysis (Goecks et al., 2010; Blankenberg et al., 2010; Giardine et al., 2005; Langille et al., 2013). PICRUSt compares 16S rRNA marker gene data to reference genomes and provides a prediction of the metagenome of a sample. Data in the biom-file was normalized with 16S rRNA gene copy number. Prediction of the functionality of the metagenome of each sample was done by multiplying the normalized abundance of each OTU by each predicted functional feature abundance. A weighted nearest sequenced taxon index (NSTI) was calculated for all samples. The NSTI value describes the average branch length that separates each OTU in the sample from a reference genome, weighted by the abundance of that OTU in the sample. For example, the NSTI value of 0.03 means that the OTUs in the sample are on average 97 % similar to the genomes in the database.

18113

In order to obtain complete metabolic pathway modules from the predicted metagenomes, the KEGG abundance data from the PICRUSt analysis was used as input for HUMAnN v. 0.99 (Abubucker et al., 2012), which was modified to include modules M00597 (Anoxygenic photosystem II), M00598 (Anoxygenic photosystem I), M00595 (Thiosulfate oxidation by SOX complex, thiosulfate => sulfate), K16952 (sulfur oxygenase/reductase), M00596 (Dissimilatory sulfate reduction, sulfate => H₂S), M00567 (Methanogenesis, CO₂ => CH₄), M00528 (Nitrification, ammonia => nitrite), and M00563 (Methanogenesis, methylamine/dimethylamine/trimethylamine => CH₄).

Co-occurrence of OTUs in total and active microbial communities of Outokumpu bedrock fractures was analyzed with the `otu.association` command in mothur. Based on pairwise Pearson correlations with significant p value (< 0.01), visualization of the co-occurrence network was constructed using Fruchtermann–Feingold layout in the Gephi program (Bastian et al., 2009). The keystone OTUs were revealed with the betweenness centrality calculation and the connectivity of the network with the closeness centrality estimate (Brandes, 2001). Modular structure of the community was evaluated with the modularity index calculation (Blondel et al., 2008; Lambiotte et al., 2009).

3 Results

3.1 Microbial density in the fracture zones

The total microbial cell numbers were highest in the 180 m fracture and declined according to the depth (Fig. 1) (Table 2). A similar trend was observed with the copy numbers of bacterial 16S rRNA gene. Archaeal 16S rRNA gene copy numbers varied more, but the highest number of archaeal 16S rRNA gene copies was detected from the fracture at 180 m depth (Table 2).

The number of *dsrB* and *mcrA* gene copies, used as an estimate for the amount of sulphate reducing bacteria and methane producing archaea, respectively, was assessed with quantitative PCR. The copy numbers were quantified also from RNA in

18114

order to estimate the activity of sulphate reduction and methanogenesis. The *dsrB* copy numbers varied between $3\text{--}6 \times 10^2$ copies mL^{-1} in most fractures with the exceptions of the 500 and 967 m fractures where the *dsrB* copy number was 7.4×10^3 and 1.5×10^1 copies mL^{-1} , respectively (Table S1 in the Supplement). As a proxy of active transcription of *dsrB* genes, the number of mRNA transcripts was also quantified. The highest *dsrB* gene transcription was observed at 1820 m, where the number of *dsrB* transcripts was more than 6.0×10^2 transcripts mL^{-1} . All other fractures had below 1.0×10^2 transcripts mL^{-1} . Methanogenesis marker gene copies were detected only from the upper three fractures (180, 500 and 967 m). The *mcrA* gene copy numbers were just above the detection limit of the assay, i.e. less than 4.0×10^1 copies mL^{-1} in all. *McrA* gene transcripts were detected only from the 967 m fracture, where the copy number was just above 1.0×10^2 mL^{-1} .

3.2 The structure of the microbial communities and correlation to geochemistry

The sequencing data acquired from DNA were used as a representation of the total microbial community present in the fracture fluid samples whereas the microbial communities derived from RNA were used as a proxy of an active community. The microbial communities differed between the nucleic acid fractions as well as the sampling depth (Fig. 2). Pyrosequencing of the total and active bacterial communities based on the 16S rRNA gene resulted to 268 identified OTUs representing a total of 157 families in six fractures analysed (Table S2). Sulfate reducing communities (based on the *dsrB* gene) were successfully sequenced from all fracture fluid samples except the active community in the 2260 m fracture and total and active communities in 2300 m. The archaeal communities were overall less diverse than the bacterial communities. Archaeal sequences (16S rRNA gene) were retrieved from all fractures except the one at 1820 m. Only 17 different OTUs could be divided to 11 families (Table S3). Total methanogen communities were detected from 180, 500, 2260 and 2300 m fractures and active methanogen communities from 500 and 967 m fractures.

18115

3.2.1 The 180 m fracture

The bacterial communities in the upmost fracture zone analysed in this study were dominated by OTUs resembling *Comamonadaceae* (Fig. 2). This β -proteobacterial family constituted over 70 % of the OTUs in total and active communities in the 180 m fracture (Table S2). The estimated richness of the community was 69 % of the observed OTUs of the 180 m bacterial communities (Table S4a). *Desulfatirhabdum* (54 % relative abundance) and *Desulfotomaculum* (98 % relative abundance) were most abundant in total and active sulfate reducing communities, respectively (Fig. 2). The archaeal community in the fracture zone at 180 m was dominated by OTUs affiliated with *Methanobacteriaceae* and *Methanoregula*, while *Methanosarcina* and methylotrophic *Methanobolus* OTUs represented minor groups (Table S3). This depth hosted the most diverse archaeal communities (the Shannon diversity index H' 2.4 and 2.1 for total and active archaeal communities, respectively) (Table S4b). Similarly, the methanogen community was the most diverse at this fracture, and the dominating groups were similar to unclassified, uncultured methanogen sequences retrieved from wetland soil (LW-25) and acidic peat bog (MB04-15a).

3.2.2 The 500 m fracture

The total bacterial community in the 500 m fracture was dominated by *Comamonadaceae* (70 %) (Fig. 2, Table S2). The dominating OTUs in active bacterial community affiliated with α -proteobacterial order *Rhodobacterales* with 38 % relative abundance, otherwise this community comprised of OTUs affiliating to *Comamonadaceae* (23 %), *Dietzia* (23 %) and *Pseudomonas* (6 %). The amount of observed OTUs captured 77–86 % richness of the communities according to the Chao1 estimate at this depth (Table S4a). *Desulfotomaculum* and *Pelotomaculum*-affiliating OTUs were the most dominant sulfate reducers in this fracture (Fig. 2). The total and active archaeal communities comprised almost solely of methanogenic *Methanobacteriaceae*, while

18116

Methanobrevibacter and *Methanosarcina* dominated the communities detected with methanogen-specific marker gene (*mcrA*) (Fig. 2).

3.2.3 The 967 m fracture

The total bacterial community in 967 m fracture zone comprised of *Natrananaerobiales*, *Clostridiales* and other *Firmicutes* in addition to mollicute *Acholeplasma*. In the active bacterial community, peptococcal *Syntrophobotulus* dominated and otherwise the community resembled the total community (Fig. 2). The observed richness was 84 or 88 % of the estimated richness of the total and active communities, respectively (Table S4a). Based on the Shannon diversity index H' (2.3) the total archaeal community in the 967 m fracture was among the most diverse of the archaeal communities. It was dominated by OTUs affiliating with SAGMEG-1 Euryarchaeota. In the active archaeal community in this fracture *Methanobacteraceae* dominated and SAGMEG OTUs represented only a minority of the OTUs. *Methanosarcina* dominated the active methanogen community in the 967 m fracture (Fig. 2).

3.2.4 The 1820 m fracture

The number of observed bacterial OTUs was among the highest in both total and active bacterial communities in the fracture zone at 1820 m. *Pseudomonadales* (29 % relative abundance), *Burkholderiales* (22 %) with *Comamonadaceae* and *Oxalobacteriaceae*, *Clostridiales* (13 %) comprised mainly of *Dethiosulfatibacter* and other *Firmicutes* with unresolved phylogeny dominated the total community in this fracture zone. In the active community OTU 86 belonging to *Firmicutes* was dominant with 39 % relative abundance (Fig. 2). The sequenced communities at this depth were estimated to have captured in average 80 % of the richness of the total communities (Table S4a). The total SRB community in this fracture was entirely composed of *Desulfovibrio*-affiliating OTU. The estimated diversity was low because only 115 sequences were retained. On the other hand, the active SRB community was diverse, with OTUs affiliating with

18117

Desulfatirhabdum, *Desulfobulbus* and *Desulfoarculus*. Amplification of archaeal and methanogen communities was not successful from this fracture indicating low abundance of these groups.

3.2.5 The 2260 m fracture

The fracture at 2260 m hosted a bacterial community mainly comprising of actinobacterial OBP41 class (53 % relative abundance) and *Burkholderiales* (34 %) (Fig. 2). The active community in this fracture had the highest amount of observed OTUs of the whole dataset and best success in capturing the richness (91 %) of the community. OTUs belonging to α -proteobacterial *Bradyrhizobium* (20 %) and *Rickettsiales* (11 %) in addition to *Firmicutes* and *Actinobacteria* dominated this active community. *Desulfotomaculum* and *Desulforudis*-affiliating OTUs dominated the total SRB community at this fracture and *Methanobacterium* dominated both archaeal and methanogen communities (Fig. 2).

3.2.6 The 2300 m fracture

The most frequent OTUs in the bacterial communities in the fracture zone at 2300 m represented *Burkholderiales* (31 % of the OTUs) and *Pseudomonadales* (25 %) such as *Moraxellaceae* and *Pseudomonadaceae*. In addition, OTUs belonging to other *Firmicutes*, *Clostridiales*, *Actinomycetales* and *Natrananaerobiales* were detected (Fig. 2). The sequenced DNA community covered 86 % of the estimated richness. The active community of this fracture mainly composed of unclassifiable OTUs: only 4 % of the community could be determined to more specifically than to phylum level, while half of the community could be determined only to phylum level (*Firmicutes*) leaving the rest of the community, 46 % unresolved. This reflected also to the richness and coverage indicator values: only 51 % of the richness was captured and the coverage was barely half (51 %) of the total abundance of the community.

18118

Sulfate reducers were not detected at this depth, and *Methanobacterium* dominated the total archaeal and methanogen communities.

3.2.7 The core microbial community in Outokumpu bedrock fractures

Only a few OTUs that were present in all communities constituted the core community in the Outokumpu deep bedrock. *Pseudomonas* and *Dethiosulfatibacter* in addition to two OTUs with uncertain taxonomic classification (Firmicutes OTU 86 and bacterial OTU1) were detected in all total and active bacterial communities. When observing only the total bacterial communities, most abundant members of the core community were *Comamonadaceae*, *Dethiobacter* and *Pseudomonas*.

3.2.8 The relationship of the microbial community structure to geochemistry

Microbial OTUs formed three loose clusters in canonical correspondence analysis based on the depth where fracture fluid samples were retrieved (Fig. 3). A cluster of bacterial OTUs belonging to orders *Burkholderiales* and *Rhodobacterales* plotted near 180 and 500 m depths and correlated with biotite gneiss and concentration of its main elemental components, iron and magnesium. Microbial OTUs affiliating with the most abundant groups in the 967 m fracture (*Peptococcaceae*, *Anaerobrancaceae*, *Thermoanaerobacterales*, SAGMEG archaea) grouped loosely around the 967 m depth with sulfur concentration pointing to this ordination. The depths of 1820 and 2300 m correlated with sulfide concentration and defining rock types were black schist and pegmatitic granite. Clostridial *Dethiosulfatibacter* and other Firmicutes-affiliating OTUs in addition to several *Burkholderiales*-affiliating OTUs clustered close to these depths.

3.3 The functionality estimation of the microbial communities

The physiology of the members of the microbial communities was estimated from classified OTUs based on the prevalent physiology of the cultured representatives of each OTU at family level according to the Prokaryotes handbook (Rosenberg et al., 2014)

18119

(Fig. 4). Bacterial physiotypes with capacity to use versatile metabolic pathways for carbon assimilation and energy production were characteristic in the fracture communities at shallower depths (180 and 500 m), while lithotrophic bacterial physiotypes are more frequently detected in 967 and 1820 m fractures. Overall, physiotypes with unknown metabolism became more frequent in the communities at fractures located deeper in the bedrock due to the lack of exact taxonomic classification of the OTUs detected in these fractures (Fig. 4a). In the archaeal communities the most dominant archaeal physiotype was hydrogenotrophic methanogenesis except in the 967 m fracture (Fig. 4b). The total archaeal community in this fracture was dominated by SAGMEG-affiliating OTUs with undetermined physiology.

3.3.1 Predicted bacterial metagenomes

The metagenomes of the microbial communities of different fracture zones representing six different biotopes were predicted from the 16S rRNA gene sequences, i.e. from the different OTUs with resolved taxonomy. In order to evaluate the accuracy of the prediction of metagenomes, nearest sequenced taxon index (NSTI) was calculated for each sample (Table S5). The NSTI's varied between the bacterial communities from 0.07 (the communities in 1820 and 2300 m fractures) to 0.30 for the community in 2260 m fracture. The archaeal communities represented NSTI's from 0.04 to 0.07 with the exception of the total community in 967 m fracture of which the NSTI was 0.29. Overall, the predicted metagenomes of the total communities did not vary greatly from the active community metagenomes. Top-level functionality estimates revealed differences between bacterial and archaeal communities. The average values for cellular processes and environmental information processing were more abundant in the predicted bacterial metagenomes than in the archaeal metagenomes. In contrast, genetic information processing and unknown features were more abundant in the predicted archaeal metagenomes (Fig. 5).

The most abundant group of bacterial predicted on the basis of PICRUSt analysis were those involved in amino acid metabolism (21–22 % of all metabolism genes),

18120

carbohydrate metabolism (19–21 %) and energy metabolism (11–13 % of all genes involved in metabolism) (Table 3a). The predicted bacterial metagenomes differed mostly between 180 m and other fractures. In all fractures, the most abundant amino acid metabolism genes were amino acid related enzymes and arginine and proline metabolism genes (11–15 % and 11–13 % respectively) (Table S6a). In the predicted bacterial metagenome in the 180 m fracture, genes involved in phenylalanine, tyrosine, tryptophan and lysine biosynthesis were more abundant than in other fractures. On the other hand, branched-chain amino acid (valine, leucine and isoleucine) degradation represented 7–11 % of the predicted amino acid metabolism genes in all other bacterial communities than those at 180 m fracture, where it was approximately only half of this (4–5 %). Gene predictions on carbohydrate utilization revealed a highly similar pattern in all other fracture communities than those at 180 m (Table S6a). Amino sugar metabolism genes were more abundant in the 180 m, while in other fractures propanoate and butanoate metabolism genes were dominant. The most abundant energy metabolism genes were involved in oxidative phosphorylation in the predicted metagenomes of the bacterial communities (22–26 % in total bacterial communities, and 20–28 % in active communities) (Table S6a). Genes involved in carbon fixation pathways in prokaryotes were almost as common, in addition to methane metabolism genes.

To evaluate the operational capacity of different metabolic pathways detected with PICRUSt, HUMAnN analysis was performed on the predicted metagenomes. Genes needed for several amino acid biosynthesis pathways and transport systems to function were present. The relative abundance of the genes involved in carbon fixation pathways such as Arnon–Buchanan, Wood–Ljungdahl and Calvin cycle were low according to the HUMAnN analysis (Table S7). Calvin cycle genes were only present in the predicted metagenomes of the active bacterial communities in 1820 and 2260 m fractures. The coverage of pathways involved in carbohydrate metabolism (KEGG modules 1–4, 6–9, 11) was high.

18121

The genes needed for coding of the enzymes in sulfur and sulphate reduction pathways were only covered in the communities in the 180 m fracture. Aerobic methane oxidation pathway on the other hand was considered operational in communities from 500 m fracture and other fractures below this (Table S7).

3.3.2 Predicted archaeal metagenomes

Similar to bacteria, half of the genes in the predicted archaeal metagenomes of each fracture zone were involved in metabolism (Fig. 5b). Energy metabolism genes were most common (18–25 %) in addition to amino acid metabolism and carbohydrate metabolism genes (21–25 and 17–20 %, respectively) (Table 3b). The predicted metagenome of the total archaeal community in the 967 m fracture zone had the highest abundance of amino acid metabolism genes (25 % of all metabolism genes) and the lowest abundance of energy metabolism genes (18 %) and thus differed from the community metagenome derived from RNA in the same fracture. Otherwise the predicted metabolism genes were similar in the different archaeal communities in the fracture zones. The predicted metagenome of the total archaeal community of the 967 m fracture differed also in predicted amino acid usage, carbohydrate metabolism and in the energy metabolism gene predictions. As expected, genes representing methane metabolism were the most dominant in all archaeal communities (Table S6b). However, oxidative phosphorylation genes were twice as frequent (16 % relative abundance) in the metagenome based on the total community in the 967 m fracture as in all other predicted metagenomes. Additionally, the community in the 180 m fracture differed from the other archaeal communities in predicted energy metabolism: less methane metabolism genes were detected in this community (61 % in the total community and 64 % in the active community), and genes involved in carbon fixation pathways were more abundant in the community in this fracture (16 % in DNA community and 14 % in RNA community).

The methanogenesis pathway from CO_2 to CH_4 was present and complete in all archaeal communities according to the HUMAnN analysis (Table S8). Methanogenesis

18122

pathway from methylamines or methanol was detected and likely operational only in the communities in the 180 m fracture.

3.4 Co-occurrence of microbial OTUs in deep crystalline bedrock

From all detected microbial OTUs in deep crystalline fractures, only 15 % showed positive correlation ($r > 0.8$) with other members of the microbial communities. Only three significantly negative correlations ($p \leq 0.01$, $r < -0.8$) were detected among the total microbial communities and none in the active communities. The network analysis of the total microbial community divided significantly correlating OTUs into 8 modules with number of nodes ranging from 4 to 41 (Fig. 6). The closeness of centrality (CC) values varied only slightly between most of the OTUs indicating that the network had high connectance between different members (variance 0.5) (Table 4). The keystone OTUs were detected based on their above 300 betweenness of centrality (BC) value and these belonged to *Burkholderiaceae*-like OTU, *Desulfitobacter* and *Clostridiaceae*-affiliating OTU, all of which had relatively low abundance (0–3%) in the communities, in addition to *Dethiobacter* with 0–5% relative abundance in other total bacterial communities except in the 967 m fracture, in which the relative abundance of this OTU in the total bacterial community was higher, 25% (Figs. 2a and 6). The most connected OTUs in the network belonged to *Rhodococcus* and *Herbaspirillum* (48 connections each) in addition to OTUs resembling *Renibacterium*, *Gemellaceae*, *Trabulsiella* and *Novosphingobium* (46–47 connections each). The positively correlating OTUs of the active microbial community divided into 8 clusters with number of nodes ranging from 2 to 64 (Fig. 7). The active community network had also small variation in the CC values (variance 0.3). The keystone genera of the active microbial community network were *Comamonas*, *Curvibacter* and *Sphingomonas*, with BC values above 470 each. *Comamonadaceae*-affiliating OTU was determined to be part of the core community in this Fennoscandian deep subsurface site, as it was frequently found in all depths with relatively high abundance ranging from 7–72% of the total community. *Curvibacter* and

18123

Sphingomonas were both present in the active communities, but with a very low relative abundance.

4 Discussion

The bacterial community structure in the Outokumpu fracture zones varies between the different depths. In addition, the structure of the total and active communities differs within the fracture zones. The core bacterial community of the deep crystalline bedrock in Outokumpu was composed of few OTUs found from all microbial communities in the fractures. Most abundant of these were *Comamonadaceae*-, *Firmicutes*-, *Anaerobrancaceae*- and *Pseudomonadaceae*-affiliating OTUs. However, the majority of the bacterial OTUs discovered in this study could be regarded as members of the so-called “rare biosphere” with their relatively low abundance and uneven distribution throughout the fracture zones (Sogin et al., 2006).

A keystone species has greater impact on its community or living environment than would be expected from its relative abundance or total biomass (Paine, 1995). Several keystone genera of both the active and the total microbial community were representatives of *Burkholderiales* (e.g. *Comamonas*, *Curvibacter*, *Oxalobacter*, *Herbaspirillum*, *Pelomonas*, *Cupriavidus*). In addition, some clostridial phylotypes were among the keystone genera. Several keystone genera detected with the co-occurrence networks were members of the rare biosphere, thus providing further evidence for the significance of the less abundant microorganisms for the whole community (Sogin et al., 2006; Brown et al., 2009). Hence, we propose that these have a major role in the functionality of the network. The metabolic flexibility of *Burkholderiales* species, for example the ability to use both autotrophic and heterotrophic carbon fixation mechanisms is beneficial in isolated deep biosphere environments where concentrations of different carbon substrates fluctuate over time (Moser et al., 2005; Magnabosco et al., 2015).

18124

4.1 Serpentinization as a source for energy in Outokumpu

Hydrogen oxidizing, facultatively chemolithotrophic members of the *Comamonadaceae*-family were dominating the 180 and 500 m fracture zone communities. These microbes are commonly found from hydrogen-enriched subsurface environments. These include findings of *Ralstonia* and *Hydrogenophaga* in Lost City Hydrothermal Field and Tablelands Ophiolite serpentinite springs, respectively (Brazelton et al., 2012, 2013). Likewise, *Comamonadaceae*-affiliating and clostridial sequences formed the majority of the bacterial community in serpentinization-driven subsurface aquifer in Portugal (Tiago and Verissimo 2013). *Comamonadaceae* were also dominant in the drill hole water communities in Outokumpu at shallow depths (0–100 m) (Itävaara et al., 2011), and at 200 and 2300 m depths (Nyyssönen et al., 2014). Additionally, *Comamonadaceae* were detected from other depths in the drill hole water column, such as at 1100–1500 m depth that was characterized by ophiolitic rock sequence (Nyyssönen et al., 2014). However, Kietäväinen et al. (2013) detected substantial amounts of H₂ only in fractures below 1500 m in Outokumpu, which might indicate that the source for H₂ for abundant hydrogen-oxidizers is in the bedrock aquifer that 180 and/or 500 m fractures intersect or lead into. The seismic reflectors of Outokumpu bedrock demonstrate ophiolite-derived rock types in the vicinity of the drill hole, some of which are located also at shallow depths (Kukkonen et al., 2011). Thus, we assume that these may affect the two shallowest fracture fluids and explain the similarity of the microbial results with other ophiolitic, serpentinizing environments.

The bacterial community of the 967 m fracture zone also resembles those of serpentinizing environments. One major member of the total bacterial community at 967 m fracture was hydrogen-oxidizing *Dethiobacter* that has previously been detected also from groundwaters associated with ophiolitic rock sequence with active serpentinization processes (Tiago and Verissimo, 2013). Brazelton et al. (2013) detected acetyl-CoA synthase gene affiliating with *Dethiobacter* from bacterial shotgun-sequenced metagenomes from bacterial Winter House Canyon (WHCB) samples from Tablelands

18125

Ophiolite. Moreover, similarities between serpentinizing environments and the deep biosphere of Outokumpu bedrock include the detection of abundant clostridial phylotypes such as *Anaerobrancaceae* from the deeper parts of the bedrock (Itävaara et al., 2011; Brazelton et al., 2013; Purkamo et al., 2013; Nyyssönen et al., 2014). The keystone species of the total and active microbial communities detected in this study reflect the similarity between the serpentinizing environments and Outokumpu deep biosphere with *Comamonadaceae*, *Burkholderiaceae*, *Clostridiaceae* and *Dethiobacter* as the recognized keystone families.

Overall, the spatial distribution of *Burkholderiales* at shallower depths and *Clostridiales* in the fractures located deeper in the bedrock can be explained to some level with the availability of electron acceptors. Both of these groups are able to use H₂ as electron donor, but *Comamonadaceae* are mainly aerobic chemoorganotrophs using a wide variety of different organic carbon compounds for energy and using oxygen as terminal electron acceptor (Willems et al., 1991), while *Dethiobacter* is a strict anaerobe that reduces sulphur compounds but not sulphate (Sorokin et al., 2008). However, as their co-occurrence in the 1820 m fracture suggests, these organisms can prevail in same environment. In Outokumpu, low concentrations of oxygen were measured during the pumping of the fracture fluids (< 0.1 mg L⁻¹) (Purkamo et al., 2013). However, it is likely that this is due to the atmospheric contamination during the measurements in the field. In addition, small amounts of oxygen can be produced in radiolysis of water in bedrock (Pedersen, 1997; Lin et al., 2005). This might explain the detection of aerobic bacteria such as *Comamonadaceae* in the deep fluids of Outokumpu.

Higher hydrogen concentration in the two deepest fracture fluids (Kietäväinen et al., 2013) could indicate that something else than the electron donor is limiting the communities at these depths. Abundant bacterial groups of the communities in the 2260 m fracture belonged to Actinobacteria and α -proteobacteria. Little is known about metabolic capacities of the OPB41 candidate phylum, but as an actinobacterial phylotype, they may be chemoorganotrophs, while *Bradyrhizobiaceae* are mixotrophs with the capacity to oxidize H₂. The fractures located below 2 km depth, mostly dominated

18126

by unclassifiable phylotypes, might suggest that these depths harbour life that differs considerably from the currently known microorganisms.

4.2 Comparison of the microbial community structure and functionality between different Precambrian deep subsurface sites

5 Bacterial and archaeal communities from the Outokumpu fracture zones resemble the drill hole water communities described in a previous study (Nyyssönen et al., 2014). This is not surprising, as drill hole fluids are a mixture of the different fracture fluids emanating to the drill hole from the fractures at different depths of the bedrock. *Comamonadaceae* form a major part of the bacterial community at most depths in the drill
10 hole, as they are abundant in 180, 500, 2260 and 2300 m fracture communities. At 967 and 1820 m fracture communities, phylotypes affiliating with *Clostridiales* are dominating, while clostridial phylotypes represent a major fraction of the drill hole communities at 1000–1500 m. Many sulfate reducer phylotypes detected in this study were similar to those detected from the drill hole fluids (Itävaara et al., 2011; Purkamo et al., 2015) and
15 from fracture zones (Purkamo et al., 2013) with DGGE. These included *Desulfotomaculum* and *Desulfovibrio*. Archaeal communities in the fractures and in the drill hole are mainly dominated by *Methanobacterium*, but SAGMEG archaea are also abundant in the drill hole communities at 1000 m and above (Nyyssönen et al., 2014), possibly originating from the 967 m fracture where SAGMEG archaea were dominating the total
20 archaeal community.

Members of *Comamonadaceae* and *Pseudomonadaceae* belong to the core microbial community in Outokumpu. These were also detected from all studied microbial communities in another Fennoscandian crystalline bedrock environment in Olkiluoto fracture zones (Bomberg et al., 2015a). To emphasize the importance of these mi-
25 crobes to the total communities in deep crystalline bedrock environments, members of *Comamonadaceae* were recognized as the keystone genera of the active microbial community in the Outokumpu deep biosphere.

18127

The microbial communities in Outokumpu deep crystalline bedrock share common features with those of the deep ecosystems in Witwatersrand Basin, South Africa. Clones affiliating with *Comamonadaceae* have been found from a deep drill hole outlet in Driefontein gold mine in South Africa. In addition, clostridial sulphate reducers, such
5 as *Desulfotomaculum*, are dominating the SRB communities in Outokumpu as well as the deep borehole communities in Driefontein (Baker et al., 2003; Moser et al., 2003, 2005; Silver et al., 2010). Candidatus *Desulforudis audaxviator* was a minor component (with 1–35 % relative abundance) of the SRB communities in Outokumpu fractures at depths of 180–2260 m, in contrast to a microbial community where *D. audaxviator*
10 formed a single-species ecosystem in deep bedrock fracture in Mponeng mine (Chivian et al., 2008). The archaeal community in the 967 m fracture was dominated by SAGMEG archaea that were first discovered from gold mines in South Africa (Takai et al., 2001). The predicted metagenome of the archaeal community at this depth showed notably higher amount of genes involved in oxidative phosphorylation than
15 other fracture communities. Whether this is a bias induced by the absence of complete genomes of closely related species in the database or an indication of oxidative phosphorylation genes having a specific role in SAGMEGs remains to be resolved. Furthermore, this study supports the biogeographical trend that methanogens in different deep Precambrian sites are similarly distributed within depth (Kietäväinen and
20 Purkamo, 2015). Methanogens with wider substrate range were found in the fractures located at shallower depths both in Outokumpu and several deep subsurface sites in South Africa. On the other hand, obligately hydrogenotrophic methanogens were detected in the fracture zones located deeper (Moser et al., 2005; Gihring et al., 2006; Lin et al., 2006). Archaeal communities represented much less diversity, and interestingly,
25 while almost all fracture zones were dominated by methanogenic archaea, the archaeal fracture community in 180 m fracture was the most diverse, where for example archaea belonging to Miscellaneous Crenarchaeal Group (MCG) and Terrestrial Miscellaneous Euryarchaeal Group (TMEG) were detected. In Olkiluoto, the highest archaeal species richness was detected from a fracture at a depth of 296 m (Bomberg

18128

et al., 2015a). In another study of archaeal communities in Olkiluoto, some indication of correlation between increasing depth and decreasing diversity could be detected (Bomberg et al., 2015b).

5 Many of the abundant bacterial groups in Outokumpu bedrock are organotrophic with capacity to use a wide range of substrates for biosynthesis and either fermentation or anaerobic respiration for energy conservation. Hence, depending on the available sources of energy and carbon, these organisms can switch to the best energy mechanism currently available. With the low relative abundance of the genes involved in autotrophic carbon fixation pathways in the predicted metagenomes, we propose
10 that in Outokumpu, heterotrophic carbon metabolism is important also for the intrinsic fracture zone communities as it is for the drill hole water column communities (Purkamo et al., 2015). Archaeal communities in Outokumpu fracture zones are mainly methanogenic, using most likely the hydrogenotrophic methanogenesis pathway from CO_2 to CH_4 .

15 5 Conclusions

The microbial communities of Outokumpu Precambrian crystalline bedrock fractures share features with serpenization-driven microbial communities in alkaline springs and subsurface aquifers. These include members belonging to *Burkholderiales* and Clostridia. Additionally, these phylotypes were regarded as the keystone species in
20 Outokumpu deep biosphere. Additionally, *Comamonadaceae* are part of the core microbial community in Fennoscandian crystalline bedrock environments. Sulfate reducing microbes and methanogens are present, but they represent marginal groups of the microbial communities. The dominating taxa of the sulphate reducing communities observed in this study are similar to the ones detected from the deep subsurface
25 of Driefontein mine in South Africa. Similarly, the total archaeal community at 967 m fracture is dominated by SAGMEG archaea, initially described at deep gold mines of South Africa. Otherwise hydrogenotrophic methanogens, mainly *Methanobacterium*,

18129

dominate the archaeal communities. The fracture zone at 180 m in Outokumpu hosts the most diverse archaeal communities. Many keystone species of Outokumpu deep biosphere belong to rare biosphere, with low abundance but a wide range of carbon substrates and a capacity for H_2 oxidation. Metagenomic predictions of the bacterial
5 communities revealed that heterotrophy is also important in the deep fracture zones in Outokumpu.

**The Supplement related to this article is available online at
doi:10.5194/bgd-12-18103-2015-supplement.**

10 *Author contributions.* L. Purkamo planned and conducted the research, analysed the data and is the corresponding author. M. Bomberg aided in planning, sampling, analysis of the data and writing the manuscript. R. Kietäväinen took part in sampling, provided hydrogeochemistry data and participated in writing the manuscript. H. Salavirta assisted in analysing the data and writing the manuscript. M. Nyyssönen took part in sampling and writing the manuscript. M. Nupponen-Puputti assisted in sampling and aided in laboratory research, L. Ahonen assisted in planning and executing the sampling and hydrogeochemistry analysis and writing the manuscript. I. Kukkonen provided access to Outokumpu Deep Drill Hole, supported sampling,
15 writing the manuscript and provided funding and M. Itävaara took part in sampling and writing the manuscript and provided funding.

20 *Acknowledgements.* Mirva Pyrhönen is acknowledged for the excellent laboratory skills and help in preparing the sampling trips. Sirpa Jylhä, Leea Ojala, Arto Pullinen and Pauliina Rajala and are acknowledged for the professional sampling assistance at the Outokumpu field site. This study was funded by Kone Foundation, The Academy of Finland (DEEP LIFE project, grant number 133348/2009), The Foundation for Research of Finnish Natural Resources (grant number 1718/09) and Finnish research program on nuclear waste management (KYT, grants
25 GEOMOL, KABIO, SALAMI and RENGAS).

References

- Abubucker, S., Segata, N., Goll, J., Schubert, A. M., Izard, J., Cantarel, B. L., Rodriguez-Mueller, B., Zucker, J., Thiagarajan, M., and Henrissat, B.: Metabolic reconstruction for metagenomic data and its application to the human microbiome, *PLoS Comput. Biol.*, 8, e1002358, doi:10.1371/journal.pcbi.1002358, 2012.
- Altschul, S. F., Gish, W., Miller, W., Myers, E. W., and Lipman, D. J.: Basic local alignment search tool, *J. Mol. Biol.*, 215, 403–410, 1990.
- Amend, J. P. and Teske, A.: Expanding frontiers in deep subsurface microbiology, *Palaeogeogr. Palaeoclimatol.*, 219, 131–155, 2005.
- Baker, B. J., Moser, D. P., MacGregor, B. J., Fishbain, S., Wagner, M., Fry, N. K., Jackson, B., Speolstra, N., Loos, S., and Takai, K.: Related assemblages of sulphate-reducing bacteria associated with ultradeep gold mines of South Africa and deep basalt aquifers of Washington State, *Environ. Microbiol.*, 5, 267–277, 2003.
- Bano, N., Ruffin, S., Ransom, B., and Hollibaugh, J. T.: Phylogenetic composition of Arctic Ocean archaeal assemblages and comparison with Antarctic assemblages, *Appl. Environ. Microbiol.*, 70, 781–789, 2004.
- Barns, S. M., Fundyga, R. E., Jeffries, M. W., and Pace, N. R.: Remarkable archaeal diversity detected in a Yellowstone National Park hot spring environment, *P. Natl. Acad. Sci. USA*, 91, 1609–1613, 1994.
- Bastian, M., Heymann, S., and Jacomy, M.: Gephi: an open source software for exploring and manipulating networks, *ICWSM*, 8, 361–362, 2009.
- Biddle, J. F., Fitz-Gibbon, S., Schuster, S. C., Brenchley, J. E., and House, C. H.: Metagenomic signatures of the Peru margin seafloor biosphere show a genetically distinct environment, *P. Natl. Acad. Sci. USA*, 105, 10583–10588, 2008.
- Biddle, J. F., White, J. R., Teske, A. P., and House, C. H.: Metagenomics of the subsurface Brazos–Trinity Basin (IODP site 1320): comparison with other sediment and pyrosequenced metagenomes, *ISME J.*, 5, 1038–1047, 2011.
- Blankenberg, D., Von Kuster, G., Coraor, N., Ananda, G., Lazarus, R., Mangan, M., Nekrutenko, A., and Taylor, J.: Galaxy: a web-based genome analysis tool for experimentalists, *Curr. Protoc. Mol. Biol.*, 19, 19.10.1–19.10.21, 2010.

18131

- Blondel, V. D., Guillaume, J.-L., Lambiotte, R., and Lefebvre, E.: Fast unfolding of communities in large networks, *J. Stat. Mech.-Theory E.*, 10, P10008, doi:10.1088/1742-5468/2008/10/P10008, 2008.
- Bomberg, M., Nyssönen, M., Nousiainen, A., Hultman, J., Paulin, L., Auvinen, P., and Itävaara, M.: Evaluation of molecular techniques in characterization of deep terrestrial biosphere, *Open J. Ecol.*, 4, 468–487, 2014.
- Bomberg, M., Nyssönen, M., Pitkänen, P., Lehtinen, A., and Itävaara, M.: Active microbial communities inhabit sulphate–methane interphase in deep bedrock fracture fluids in Olkiluoto, Finland, *BioMed Research International*, 979530, doi:10.1155/2015/979530, 2015a.
- Bomberg, M., Lamminmäki, T., and Itävaara, M.: Estimation of microbial metabolism and co-occurrence patterns in fracture groundwaters of deep crystalline bedrock at Olkiluoto, Finland, *Biogeosciences Discuss.*, 12, 13819–13857, doi:10.5194/bgd-12-13819-2015, 2015b.
- Brandes, U.: A faster algorithm for betweenness centrality, *J. Math. Sociol.*, 25, 163–177, 2001.
- Brazelton, W. J., Nelson, B., and Schrenk, M. O.: Metagenomic evidence for H₂ oxidation and H₂ production by serpentinite-hosted subsurface microbial communities, *Front. Microbiol.*, 2, 268, doi:10.3389/fmicb.2011.00268, 2012.
- Brazelton, W. J., Morrill, P. L., Szponar, N., and Schrenk, M. O.: Bacterial communities associated with subsurface geochemical processes in continental serpentinite springs, *Appl. Environ. Microbiol.*, 79, 3906–3916, doi:10.1128/AEM.00330-13, 2013.
- Brown, M. V., Philip, G. K., Bunge, J. A., Smith, M. C., Bissett, A., Lauro, F. M., Fuhrman, J. A., and Donachie, S. P.: Microbial community structure in the North Pacific ocean, *ISME J.*, 3, 1374–1386, doi:10.1038/ismej.2009.86, 2009.
- Caporaso, J. G., Kuczynski, J., Stombaugh, J., Bittinger, K., Bushman, F. D., Costello, E. K., Fierer, N., Pena, A. G., Goodrich, J. K., and Gordon, J. I.: QIIME allows analysis of high-throughput community sequencing data, *Nat. Methods*, 7, 335–336, 2010.
- Chivian, D., Brodie, E. L., Alm, E. J., Culley, D. E., Dehal, P. S., DeSantis, T. Z., Gihring, T. M., Lapidus, A., Lin, L. H., Lowry, S. R., Moser, D. P., Richardson, P. M., Southam, G., Wanger, G., Pratt, L. M., Andersen, G. L., Hazen, T. C., Brockman, F. J., Arkin, A. P., and Ostroff, T. C.: Environmental genomics reveals a single-species ecosystem deep within Earth, *Science*, 322, 275–278, doi:10.1126/science.1155495, 2008.
- Edwards, U., Rogall, T., Blocker, H., Emde, M., and Bottger, E. C.: Isolation and direct complete nucleotide determination of entire genes. Characterization of a gene coding for 16S ribosomal RNA, *Nucleic Acids Res.*, 17, 7843–7853, 1989.

18132

- Etiopo, G. and Sherwood Lollar, B.: Abiotic methane on Earth, *Rev. Geophys.*, 51, 276–299, 2013.
- Fish, J. A., Chai, B., Wang, Q., Sun, Y., Brown, C. T., Tiedje, J. M., and Cole, J. R.: FunGene: the functional gene pipeline and repository, *Front. Microbiol.*, 4, 291, doi:10.3389/fmicb.2013.00291, 2013.
- 5 Geets, J., Borremans, B., Diels, L., Springael, D., Vangronsveld, J., van der Lelie, D., and Vanbroekhoven, K.: *DsrB* gene-based DGGE for community and diversity surveys of sulfate-reducing bacteria, *J. Microbiol. Meth.*, 66, 194–205, 2006.
- Giardine, B., Riemer, C., Hardison, R. C., Burhans, R., Elnitski, L., Shah, P., Zhang, Y., Blankenberg, D., Albert, I., Taylor, J., Miller, W., Kent, W. J., and Nekrutenko, A.: Galaxy: A platform for interactive large-scale genome analysis, *Genome Res.*, 15, 1451–1455, 2005.
- 10 Gihring, T., Moser, D., Lin, L. H., Davidson, M., Onstott, T., Morgan, L., Milleson, M., Kieft, T., Trimarco, E., and Balkwill, D.: The distribution of microbial taxa in the subsurface water of the Kalahari Shield, South Africa, *Geomicrobiol. J.*, 23, 415–430, 2006.
- 15 Goecks, J., Nekrutenko, A., Taylor, J., and The Galaxy Team: Galaxy: a comprehensive approach for supporting accessible, reproducible, and transparent computational research in the life sciences, *Genome Biol.*, 11, R86, doi:10.1186/gb-2010-11-8-r86, 2010.
- Gold, T.: The deep, hot biosphere, *P. Natl. Acad. Sci. USA*, 89, 6045–6049, 1992.
- Grosskopf, R., Janssen, P. H., and Liesack, W.: Diversity and structure of the methanogenic community in anoxic rice paddy soil microcosms as examined by cultivation and direct 16S rRNA gene sequence retrieval, *Appl. Environ. Microb.*, 64, 960–969, 1998.
- 20 Hales, B. A., Edwards, C., Ritchie, D. A., Hall, G., Pickup, R. W., and Saunders, J. R.: Isolation and identification of methanogen-specific DNA from blanket bog peat by PCR amplification and sequence analysis, *Appl. Environ. Microb.*, 62, 668–675, 1996.
- 25 Hallbeck, L. and Pedersen, K.: Characterization of microbial processes in deep aquifers of the Fennoscandian Shield, *Appl. Geochem.*, 23, 1796–1819, 2008.
- Hallbeck, L. and Pedersen, K.: Culture-dependent comparison of microbial diversity in deep granitic groundwater from two sites considered for a Swedish final repository of spent nuclear fuel, *FEMS Microbiol. Ecol.*, 81, 66–77, 2012.
- 30 Hammer, Ø., Harper, D., and Ryan, P.: Past: paleontological statistics software package for education and data analysis, *Paleontología Electrónica*, 4, 1–9, available at: http://palaeo-electronica.org/2001_1/past/past.pdf (last access: 6 November 2015), 2001.

18133

- Itävaara, M., Nyssönen, M., Kapanen, A., Nousiainen, A., Ahonen, L., and Kukkonen, I.: Characterization of bacterial diversity to a depth of 1500 m in the Outokumpu Deep Borehole, Fennoscandian Shield, *FEMS Microbiol. Ecol.*, 77, 295–309, 2011.
- Kietäväinen, R. and Purkamo, L.: The origin, source and cycling of methane in deep crystalline rock biosphere, *Frontiers in Microbiology*, 6, 725, doi:10.3389/fmicb.2015.00725, 2015.
- 5 Kietäväinen, R., Ahonen, L., Kukkonen, I. T., Hendriksson, N., Nyssönen, M., and Itävaara, M.: Characterisation and isotopic evolution of saline waters of the Outokumpu Deep Drill Hole, Finland – Implications for water origin and deep terrestrial biosphere, *Appl. Geochem.*, 32, 37–51, 2013.
- 10 Kukkonen, I. T., Rath, V., Kivekäs, L., Šafanda, J., and Čermák, V.: Geothermal studies of the Outokumpu Deep Drill Hole, in: *Outokumpu Deep Drilling Project 2003–2010*, edited by: Kukkonen, I. T., Geological Survey of Finland, Finland, Special Paper 51, 181–198, 2011.
- Lambiotte, R., Delvenne, J.-C., and Barahona, M.: Laplacian Dynamics and Multiscale Modular Structure, Networks, Laplacian dynamics and multiscale modular structure in networks, arXiv:0812.1770v3, 2009.
- 15 Langille, M. G., Zaneveld, J., Caporaso, J. G., McDonald, D., Knights, D., Reyes, J. A., Clemente, J. C., Burkepile, D. E., Thurber, R. L. V., and Knight, R.: Predictive functional profiling of microbial communities using 16S rRNA marker gene sequences, *Nat. Biotechnol.*, 31, 814–821, 2013.
- 20 Lau, M. C., Cameron, C., Magnabosco, C., Brown, C. T., Schilkey, F., Grim, S., Hendrickson, S., Pullin, M., Lollar, B. S., and van Heerden, E.: Phylogeny and phylogeography of functional genes shared among seven terrestrial subsurface metagenomes reveal N-cycling and microbial evolutionary relationships, *Frontiers in Microbiology*, 5, 531, doi:10.3389/fmicb.2014.00531, 2014.
- 25 Lin, L., Hall, J., Lippmann-Pipke, J., Ward, J. A., Sherwood Lollar, B., DeFlaun, M., Rothmel, R., Moser, D., Gihring, T. M., and Mislowski, B.: Radiolytic H₂ in continental crust: nuclear power for deep subsurface microbial communities, *Geochem. Geophys. Geosy.*, 6, Q07003, doi:10.1029/2004GC000907, 2005.
- 30 Lin, L., Hall, J., Onstott, T., Gihring, T., Lollar, B. S., Boice, E., Pratt, L., Lippmann-Pipke, J., and Bellamy, R. E.: Planktonic microbial communities associated with fracture-derived groundwater in a deep gold mine of South Africa, *Geomicrobiol. J.*, 23, 475–497, 2006.
- Lupatini, M., Suleiman, A. K., Jacques, R. J., Antonioli, Z. I., de Siqueira Ferreira, A., Kuramae, E. E., and Roesch, L. F.: Network topology reveals high connectance levels

18134

- and few key microbial genera within soils, *Frontiers in Environmental Science*, 2, 10, doi:10.3389/fenvs.2014.00010, 2014.
- Magnabosco, C., Ryan, K., Lau, M. C., Kuloyo, O., Sherwood Lollar, B., Kieft, T. L., van Heerden, E., and Onstott, T.: A metagenomic window into carbon metabolism at 3 km depth in Precambrian continental crust, *ISME J.*, in press, doi:10.1038/ismej.2015.150, 2015.
- McCollom, T. M.: Laboratory simulations of abiotic hydrocarbon formation in Earth's deep subsurface, *Rev. Mineral. Geochem.*, 75, 467–494, doi:10.2138/rmg.2013.75.15, 2013.
- McCollom, T. M., Lollar, B. S., Lacrampe-Couloume, G., and Seewald, J. S.: The influence of carbon source on abiotic organic synthesis and carbon isotope fractionation under hydrothermal conditions, *Geochim. Cosmochim. Ac.*, 74, 2717–2740, 2010.
- Moser, D., Onstott, T., Fredrickson, J., Brockman, F., Balkwill, D., Drake, G., Pfiffner, S., White, D., Takai, K., and Pratt, L.: Temporal shifts in microbial community structure and geochemistry of an ultradeep South African gold mine borehole, *Geomicrobiol. J.*, 20, 517–548, 2003.
- Moser, D. P., Gihring, T. M., Brockman, F. J., Fredrickson, J. K., Balkwill, D. L., Dollhopf, M. E., Lollar, B. S., Pratt, L. M., Boice, E., Southam, G., Wanger, G., Baker, B. J., Pfiffner, S. M., Lin, L. H., and Onstott, T. C.: *Desulfotomaculum* and *Methanobacterium* spp. dominate a 4- to 5-kilometer-deep fault, *Appl. Environ. Microb.*, 71, 8773–8783, 2005.
- Mu, A., Boreham, C., Leong, H. X., Haese, R. R., and Moreau, J. W.: Changes in the deep subsurface microbial biosphere resulting from a field-scale CO₂ geosequestration experiment, *Frontiers in Microbiology*, 5, 209, doi:10.3389/fmicb.2014.00209, 2014.
- Muyzer, G., de Waal, E. C., and Uitterlinden, A. G.: Profiling of complex microbial populations by denaturing gradient gel electrophoresis analysis of polymerase chain reaction-amplified genes coding for 16S rRNA, *Appl. Environ. Microb.*, 59, 695–700, 1993.
- Nyyssönen, M., Bomberg, M., Kapanen, A., Nousiainen, A., Pitkänen, P., and Itävaara, M.: Methanogenic and sulphate-reducing microbial communities in deep groundwater of crystalline rock fractures in Olkiluoto, Finland, *Geomicrobiol. J.*, 29, 863–878, 2012.
- Nyyssönen, M., Hultman, J., Ahonen, L., Kukkonen, I., Paulin, L., Laine, P., Itävaara, M., and Auvinen, P.: Taxonomically and functionally diverse microbial communities in deep crystalline rocks of the Fennoscandian shield, *ISME J.*, 8, 126–138, 2013.
- Osburn, M. R., LaRowe, D. E., Momper, L. M., and Amend, J. P.: Chemolithotrophy in the continental deep subsurface: Sanford Underground Research Facility (SURF), USA, *Frontiers in Microbiology*, 5, 610, doi:10.3389/fmicb.2014.00610, 2014.

18135

- Paine, R. T.: A conversation on refining the concept of keystone species, *Conserv. Biol.*, 9, 962–964, 1995.
- Pedersen, K.: Investigations of subterranean bacteria in deep crystalline bedrock and their importance for the disposal of nuclear waste, *Can. J. Microbiol.*, 42, 382–391, 1996.
- Pedersen, K.: Microbial life in deep granitic rock, *FEMS Microbiol. Rev.*, 20, 399–414, 1997.
- Pedersen, K.: Exploration of deep intraterrestrial microbial life: current perspectives, *FEMS Microbiol. Lett.*, 185, 9–16, 2000.
- Pedersen, K., Arlinger, J., Eriksson, S., Hallbeck, A., Hallbeck, L., and Johansson, J.: Numbers, biomass and cultivable diversity of microbial populations relate to depth and borehole-specific conditions in groundwater from depths of 4–450 m in Olkiluoto, Finland, *ISME J.*, 2, 760–775, 2008.
- Power, M. E., Tilman D., Estes, J. A., Menge, B. A., Bond, W. J., Mills, L. S., Gretchen, D., Castilla, J. C., Lubchenco, J., and Paine, R. T.: Challenges in the quest for keystones, *BioScience*, 4, 609–620, 1996.
- Proskurowski, G., Lilley, M. D., Seewald, J. S., Fruh-Green, G. L., Olson, E. J., Lupton, J. E., Sylva, S. P., and Kelley, D. S.: Abiogenic hydrocarbon production at lost city hydrothermal field, *Science*, 319, 604–607, doi:10.1126/science.1151194, 2008.
- Purkamo, L., Bomberg, M., Nyyssönen, M., Kukkonen, I., Ahonen, L., Kietäväinen, R., and Itävaara, M.: Dissecting the deep biosphere: retrieving authentic microbial communities from packer-isolated deep crystalline bedrock fracture zones, *FEMS Microbiol. Ecol.*, 85, 324–337, 2013.
- Purkamo, L., Bomberg, M., Nyyssönen, M., Kukkonen, I., Ahonen, L., and Itävaara, M.: Heterotrophic communities supplied by ancient organic carbon predominate in deep Fennoscandian bedrock fluids, *Microb. Ecol.*, 69, 319–332, 2015.
- Quince, C., Lanzén, A., Curtis, T. P., Davenport, R. J., Hall, N., Head, I. M., Read, L. F., and Sloan, W. T.: Accurate determination of microbial diversity from 454 pyrosequencing data, *Nature Meth.*, 6, 639–641, 2009.
- Rosenberg, E., DeLong, E. F., Lory, S., Stackebrandt, E., and Thompson, F. (Eds): *The Prokaryotes*, 4th Edn., Springer-Verlag Berlin Heidelberg, 2014.
- Schloss, P. D., Westcott, S. L., Ryabin, T., Hall, J. R., Hartmann, M., Hollister, E. B., Lesniewski, R. A., Oakley, B. B., Parks, D. H., and Robinson, C. J.: Introducing mothur: open-source, platform-independent, community-supported software for describing and comparing microbial communities, *Appl. Environ. Microbiol.*, 75, 7537–7541, 2009.

18136

- Silver, B., Onstott, T., Rose, G., Lin, L. H., Ralston, C., Sherwood-Lollar, B., Pfiffner, S., Kieft, T., and McCuddy, S.: In situ cultivation of subsurface microorganisms in a deep mafic sill: implications for SLiMEs, *Geomicrobiol. J.*, 27, 329–348, 2010.
- Sogin, M. L., Morrison, H. G., Huber, J. A., Mark Welch, D., Huse, S. M., Neal, P. R., Arrieta, J. M., and Herndl, G. J.: Microbial diversity in the deep sea and the underexplored “rare biosphere”, *P. Natl. Acad. Sci. USA*, 103, 12115–12120, 2006.
- Stahl, A. and Amann, R.: Development and application of nucleic acid probes, in: *Nucleic acid techniques in bacterial systematics*, edited by: Stackebrandt, E. and Goodfellow, M., John Wiley & Sons, Chichester, 205–248, 1991.
- Szponar, N., Brazelton, W. J., Schrenk, M. O., Bower, D. M., Steele, A., and Morrill, P. L.: Geochemistry of a continental site of serpentinization, the Tablelands Ophiolite, Gros Morne National Park: a Mars analogue, *Icarus*, 224, 286–296, 2013.
- Tiago, I. and Verissimo, A.: Microbial and functional diversity of a subterrestrial high pH groundwater associated to serpentinization, *Environ. Microbiol.*, 15, 1687–1706, 2013.
- Wagner, M., Roger, A. J., Flax, J. L., Brusseau, G. A., and Stahl, D. A.: Phylogeny of dissimilatory sulfite reductases supports an early origin of sulfate respiration, *J. Bacteriol.*, 180, 2975–2982, 1998.
- Willems, A., De Ley, J., Gillis, M., and Kersters, K.: Comamonadaceae, a new family encompassing the acidovorans rRNA complex, including *Variovorax paradoxus* gen. nov., comb. nov. for *Alcaligenes paradoxus* (Davis 1969), *Int. J. Syst. Bacteriol.*, 41, 445–450, 1991.
- Zhou, J., Deng, Y., Luo, F., He, Z., and Yang, Y.: Phylogenetic molecular ecological network of soil microbial communities in response to elevated CO₂, *MBio*, 2, e00122-11, doi:10.1128/mBio.00122-11, 2011.

18137

Table 1. Hydrogeochemical characteristics of six fracture zones of Outokumpu. Concentrations for cations and anions are given in mg mL⁻¹, EC in mS m⁻¹ and alkalinity in mmol mL⁻¹.

Depth m	Prevalent rock type	Ca	Fe	Mg	Na	S	Br	Cl	SO ₄	NO ₃	Sulfide	TOC	DOC	TIC	DIC	pH	EC ¹	Alkalinity
180	Mica schist, biotite gneiss	1060	0.34	16.7	1070	1.27	23	3280	1.5	< 20	0.057	12.8	9	0.7	0.6	7.4	1060	0.31
500	Chlorite- sericite schist	2250	< 0.03	12.9	1810	3.49	< 50	8180	1.0	< 100	bd	bd	bd	bd	bd	8.3	1900	0.19
967	Mica schist, chlorite- sericite schist	2000	< 0.03	0.8	1770	17.1	62.2	5790	0.6	< 40	bd	6.93	6.4	< 0.2	< 0.2	8.9	1740	0.29
1820	Mica and black schist, granite	11800	0.03	15.1	3820	44.4	159	30300	2.6	< 200	0.87	30.33	29.7	0.4	0.51	9.0	6930	0.37
2260	Biotite gneiss	8130	0.03	21	2630	4.8	< 1000	16400	< 2	< 2000	bd	bd	bd	bd	bd	8.2	4890	0.25
2300	Mica schist, granite	9480	< 0.03	18.7	3120	7.42	123	24500	< 2	< 200	0.086	34.33	34	0.4	< 0.2	8.6	4370	0.29

¹ Kietäväinen et al. (2013).

² Electrical conductivity at 25 °C.
bd = below detection limit.

18138

Table 2. The total number of cells and the 16S rRNA gene copy numbers of microbial communities in six fractures of Outokumpu. Values are given in mL⁻¹.

Fracture depth <i>m</i>	Total cell amount		Bacterial 16S rRNA gene		Archaeal 16S rRNA gene	
	cell number	SEM*	copy number	SEM*	copy number	SEM*
180	2.97×10^5	6.25×10^4	5.13×10^6	1.49×10^5	6.24×10^3	1.25×10^0
500	5.72×10^4	3.04×10^3	1.88×10^6	2.99×10^5	8.62×10^1	1.23×10^0
967	1.00×10^4	8.91×10^2	1.26×10^5	2.15×10^4	4.90×10^2	1.24×10^0
1820	4.74×10^3	1.17×10^3	9.05×10^2	2.29×10^1	bd	NA
2260	1.51×10^3	3.52×10^2	9.01×10^2	3.72×10^1	2.32×10^1	1.07×10^0
2300	6.30×10^3	1.89×10^3	9.00×10^2	2.07×10^1	bd	NA

* SEM = standard error of mean.

bd = below detection limit.

NA = not available.

18139

Table 3. The most abundant metabolism-related (a) bacterial and (b) archaeal genes in the predicted metagenomes.

(a)	180 m		500 m		967 m		1820 m		2260 m		2300 m	
	DNA	RNA	DNA	RNA	DNA	RNA	DNA	RNA	DNA	RNA	DNA	RNA
Carbohydrate Metabolism	19%	21%	20%	19%	20%	19%	19%	20%	21%	19%	19%	19%
Amino Acid Metabolism	21%	21%	22%	23%	22%	22%	21%	22%	21%	21%	22%	21%
Energy Metabolism	13%	13%	12%	11%	11%	13%	11%	12%	13%	13%	11%	11%
Metabolism of Cofactors and Vitamins	9%	0%	9%	9%	8%	10%	8%	8%	9%	8%	8%	9%
Lipid Metabolism	6%	0%	7%	8%	8%	7%	8%	8%	7%	7%	8%	7%
Nucleotide Metabolism	8%	0%	7%	6%	7%	8%	6%	7%	7%	7%	6%	8%
Xenobiotics Biodegradation and Metabolism	4%	0%	7%	8%	7%	6%	9%	6%	7%	9%	9%	7%
Metabolism of Terpenoids and Polyketides	4%	0%	4%	5%	5%	4%	4%	4%	5%	5%	4%	4%
Metabolism of Other Amino Acids	4%	0%	4%	4%	4%	3%	4%	4%	4%	4%	4%	4%
Enzyme Families	4%	0%	3%	3%	4%	4%	4%	4%	3%	3%	4%	4%
Glycan Biosynthesis and Metabolism	7%	0%	3%	3%	4%	4%	4%	3%	3%	3%	4%	4%
Biosynthesis of Other Secondary Metabolites	2%	0%	2%	2%	2%	2%	1%	1%	1%	2%	2%	1%
(b)	180 m		500 m		967 m		1820 m		2260 m		2300 m	
	DNA	RNA	DNA	RNA	DNA	RNA	DNA	RNA	DNA	RNA	DNA	RNA
Energy Metabolism	23%	23%	25%	25%	18%	24%			24%	24%	24%	
Amino Acid Metabolism	21%	21%	21%	21%	25%	22%			22%	22%	22%	
Carbohydrate Metabolism	18%	20%	17%	17%	19%	17%			17%	17%	17%	
Nucleotide Metabolism	11%	10%	11%	11%	13%	11%			11%	11%	11%	
Metabolism of Cofactors and Vitamins	10%	10%	11%	11%	10%	10%			10%	10%	10%	
Xenobiotics Biodegradation and Metabolism	3%	4%	3%	3%	2%	3%			3%	3%	3%	
Enzyme Families	3%	3%	3%	3%	3%	3%	nd	nd	3%	3%	3%	nd
Metabolism of Terpenoids and Polyketides	3%	3%	3%	3%	3%	3%			3%	3%	3%	
Glycan Biosynthesis and Metabolism	2%	2%	3%	3%	2%	2%			2%	2%	2%	
Biosynthesis of Other Secondary Metabolites	2%	2%	2%	2%	2%	2%			2%	2%	2%	
Lipid Metabolism	2%	1%	1%	1%	2%	1%			1%	1%	1%	
Metabolism of Other Amino Acids	1%	1%	1%	1%	1%	1%			1%	1%	1%	

nd = not detected.

18140

Table 4. The keystone genera of the total microbial communities in Outokumpu fractures.

Keystone OTUs	Closeness Centrality	Betweenness Centrality	Degree	Family	Relative abundance*
Other <i>Burkholderiaceae</i>	2.0	394	41	<i>Burkholderiaceae</i>	1 %
<i>Desulfitobacter</i>	2.4	302	4	<i>Peptococcaceae</i>	6 %
Other <i>Clostridiaceae</i>	1.7	302	20	<i>Clostridiaceae</i>	2 %
<i>Dethiobacter</i>	2.4	302	26	<i>Anaerobranaceae</i>	25 %
<i>Herbaspirillum</i>	1.8	248	48	<i>Oxalobacteraceae</i>	6 %
<i>Pelomonas</i>	1.8	218	41	<i>Comamonadaceae</i>	72 %
<i>Novosphingobium</i>	1.1	162	46	<i>Sphingomonadaceae</i>	2 %
<i>Comamonas</i>	1.8	151	29	<i>Comamonadaceae</i>	72 %
Average	1.4	21	25		

* Highest relative abundance in the family level in the community.

18141

Table 5. The keystone genera of the active microbial communities in Outokumpu fractures.

Keystone OTUs	Closeness Centrality	Betweenness Centrality	Degree	Family	Relative abundance ^a
<i>Curvibacter</i>	1.8	797	41	<i>Comamonadaceae</i>	71 %
<i>Comamonas</i>	1.8	476	4	<i>Comamonadaceae</i>	71 %
<i>Sphingomonas</i>	1.7	474	20	<i>Sphingomonadaceae</i>	0.1 %
<i>Bacilli</i> OTU87	1.1	294	26	<i>Bacilli</i> ^b	1 %
<i>Flavobacterium</i>	1.8	276	48	<i>Flavobacteraceae</i>	< 0,1 %
<i>Williamsia</i>	1.1	256	41	<i>Williamsiaceae</i>	< 0,1 %
<i>Staphylococcus</i>	2.5	189	46	<i>Staphylococcaceae</i>	1 %
<i>Oxalobacteraceae</i>	1.8	172	29	<i>Oxalobacteraceae</i>	0.3 %
<i>Herbaspirillum</i>	1.9	155	57	<i>Oxalobacteraceae</i>	0.3 %
Average	1.3	21	37		

^a Highest relative abundance in the family level in the community.

^b Only identified to class level.

18142

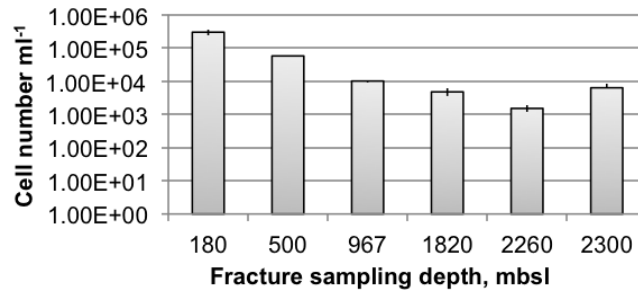
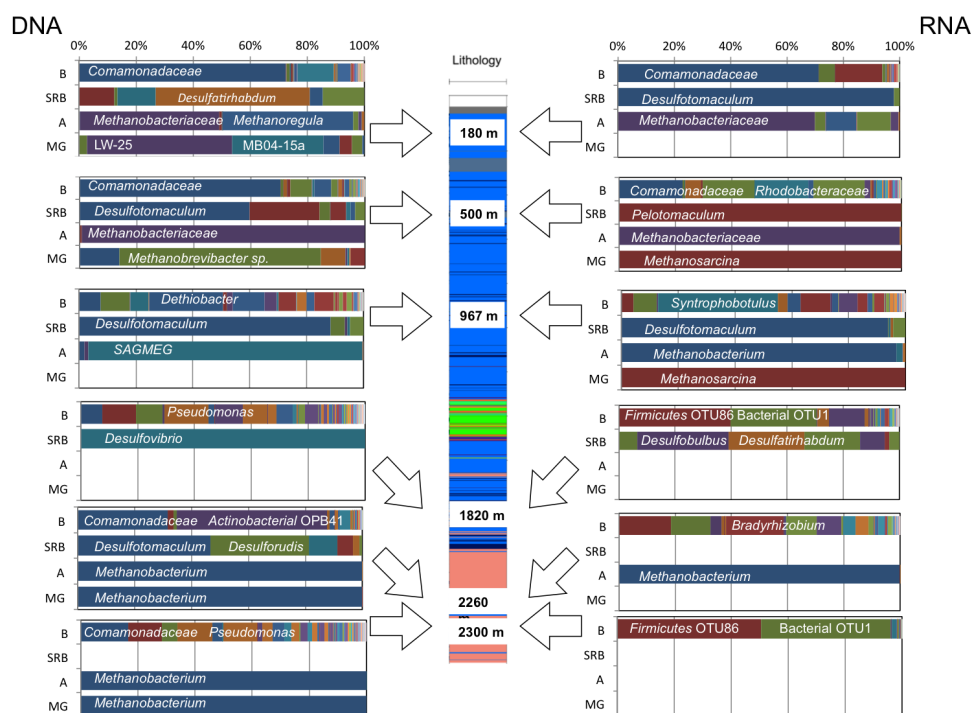


Figure 1. Total number of microbial cells in Outokumpu fracture fluids.

18143



18144

Figure 2. Microbial community structure at six different fractures in Outokumpu Precambrian crystalline bedrock. On the center a schematic presentation of the Outokumpu Deep Drill hole lithology (blue mica schist, green ophiolitic rocks, pink pegmatitic granite) with arrows pointing to the depths of the fractures studied. The composition of the total communities on the left and the active communities on the right side. The taxonomic classification of only the most abundant OTUs is shown. B: bacteria, SRB: sulphate reducing bacteria, A: archaea, MG: methanogens.

18145

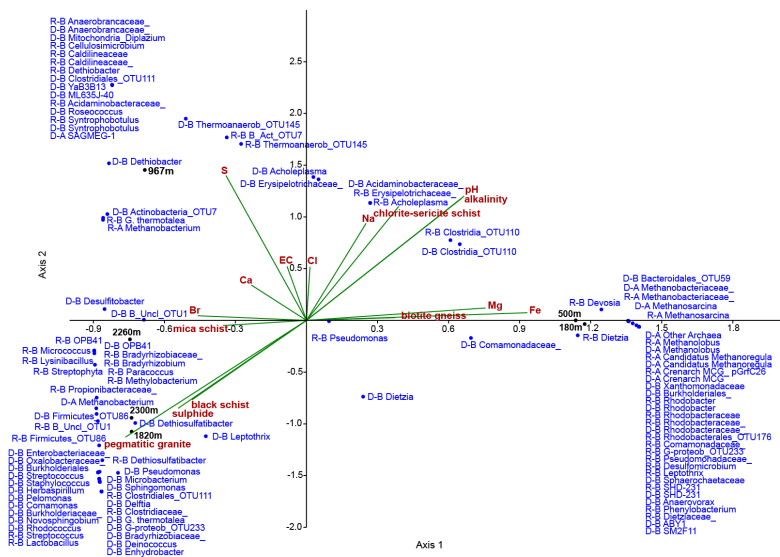


Figure 3. Canonical correspondence plot of the microbial OTUs (blue, letters before the OTU name denoting the origin and the domain, i.e. D: derived from DNA, R: derived from RNA, B: Bacteria, A: Archaea), depths (black) and the geochemical parameters (red). Horizontal axis explains the 35 % of the variance of the data with statistical significance ($p < 0.01$), as vertical axis explains 27 % of the variance of the data ($p = 0.11$).

18146

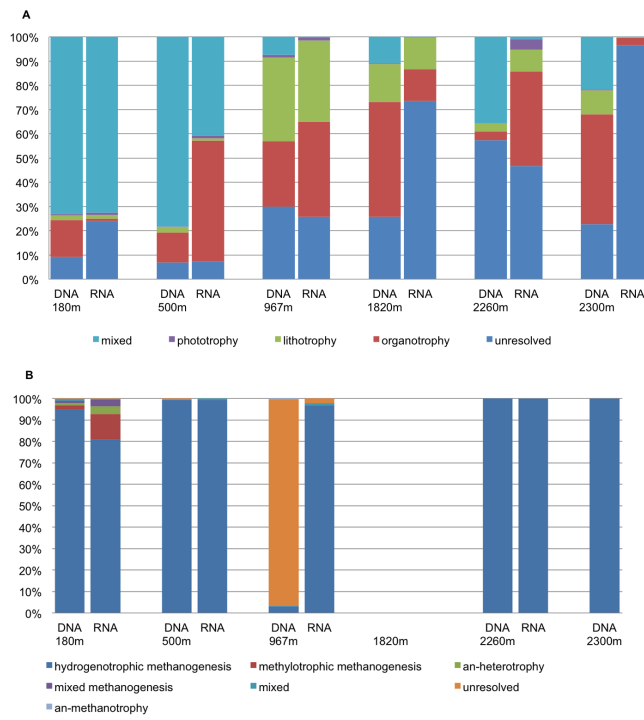


Figure 4. Binned (a) bacterial and (b) archaeal physiotypes according to the predominant metabolism of OTUs in the family level.

18147

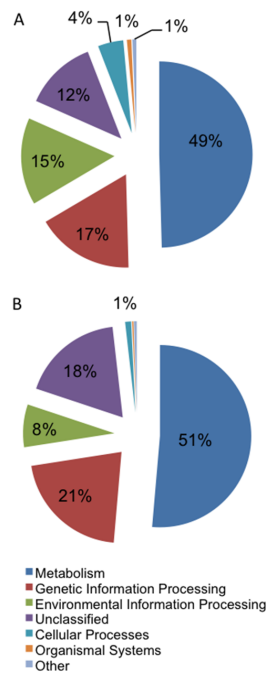


Figure 5. The average predicted functionality of all (a) bacterial and (b) archaeal metagenomes reconstructed from 16S rRNA gene sequences.

18148

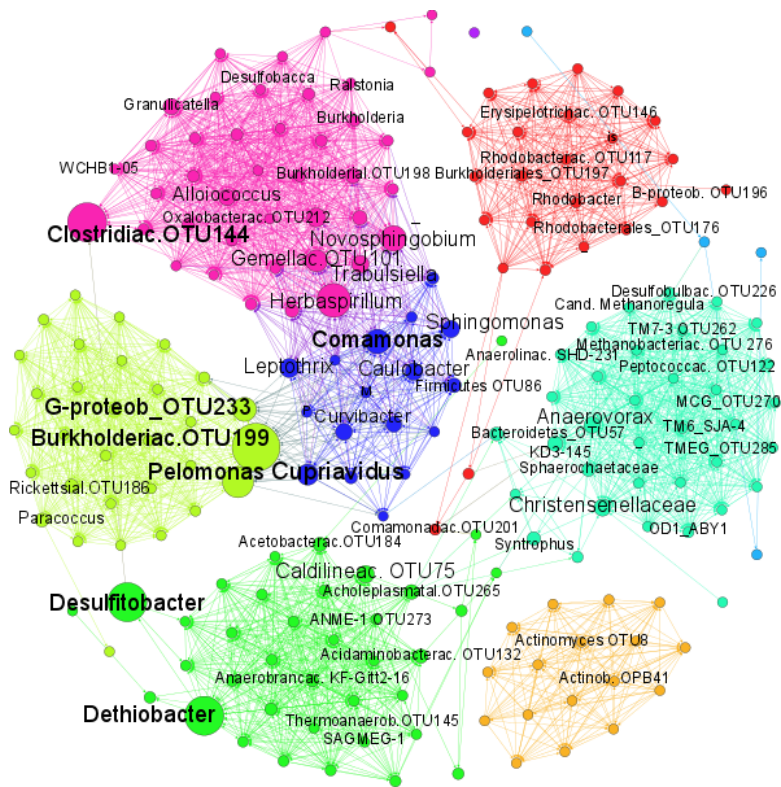


Figure 6. The co-occurrence network of the total microbial community in Outokumpu bedrock. The size of each node corresponds to the betweenness of centrality value of the OTU. The different modules are represented in different colours.

18149

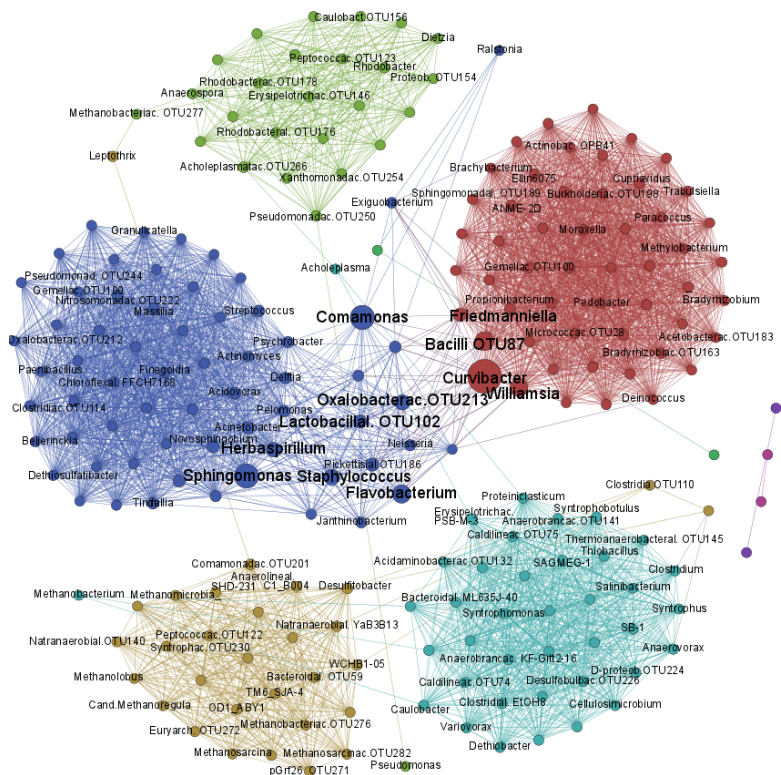


Figure 7. The co-occurrence network of the active microbial community in Outokumpu bedrock. The size of each node corresponds to the betweenness of centrality value of the OTU. Modules are represented by different colors.

18150